Design of shifting output-feedback controllers for LPV systems subject to time-varying saturations [*]

Adrián Ruiz [*] Damiano Rotondo [**] Bernardo Morcego [*]

[*] *Research Center for Supervision, Safety and Automatic Control, Universitat Politècnica de Catalunya (UPC), Rambla Sant Nebridi, 22, 08222 Terrassa, Spain. e-mails: adrian.ruiz.royo@upc.edu & bernardo.morcego@upc.edu*
[**] *Department of Electrical and Computer Engineering (IDE), University of Stavanger (UiS), Kristine Bonnevies vei 22, 4021 Stavanger, Norway. e-mail: damiano.rotondo@uis.no*

Abstract: This paper considers the problem of designing a shifting output-feedback controller for polytopic linear parameter-varying (LPV) systems subject to time-varying saturations. By means of the LPV framework and the use of the Lyapunov theory, the shifting paradigm concept, and the ellipsoidal invariant theory, a linear matrix inequality (LMI)-based methodology for the controller's design is proposed. The resulting gain-scheduled controller holds the control action in the linearity region of the actuators and regulates online the closed-loop convergence taking into account the instantaneous saturation limit values. The proposed approach is validated by means of an illustrative example.

Keywords: Linear parameter-varying (LPV), Saturation, Linear matrix inequalities (LMIs)

1. INTRODUCTION

The saturation phenomenon is always present in all real-world systems due to the actuators' inherent physical limitations. It is widely known that the saturation phenomenon can produce significant performance degradation or even destabilize the closed-loop system if it is not taken into account properly in the controller's design stage. Due to the importance of the saturation phenomenon, several researchers have investigated the design of nonlinear controllers for a long time through the application of two main popular approaches: anti-windup compensation (da Silva and Tarbouriech, 2005; Ungurán et al., 2019), where a pre-designed controller is combined with a compensator to handle the saturation; and direct control design (Kapila et al., 2001; Cao et al., 2002), in which saturation nonlinearities are directly considered in the controller design stage. Previous works in the literature have addressed, mostly, the saturation phenomenon under the common assumption of considering constant saturation limits, see e.g. Wu et al. (2000); Scorletti et al. (2001); Nguyen et al. (2018); de Souza et al. (2021).

Nevertheless, the presence of time-varying saturations in real-world systems should be considered during the controller design stage as a consequence of the natural wear of actuators or the existence of time-varying conditions. For example, in autonomous aerial vehicles, the progressive lack of energy availability can affect the available actuator action (Hoffmann et al., 2007; Faessler et al., 2017; Abdilla et al., 2015). In recent years, a few theoretical works have proposed a design methodology of gain-scheduled state-feedback controllers for linear parameter-varying (LPV) systems subject to time-varying saturations through the use of linear matrix inequalities (LMIs) and the use of the *shifting paradigm concept* presented in Rotondo et al. (2015). For instance, a *shifting* feedback controller has been developed for an N-DoF robotic manipulator in San-Miguel et al. (2021), where the closed-loop response was modified through the placement of closed-loop poles in order to avoid the actuator saturation when actively compensated effects tend to the input limits. Furthermore, a *shifting* state-feedback controller has been designed for polytopic LPV systems subject to time-varying saturation via parameter-independent and parameter-dependent quadratic Lyapunov functions (QLFs) in Ruiz et al. (2019) and Ruiz et al. (2021), respectively, with the ability to regulate online the closed-loop convergence speed according to the instantaneous saturation limit values.

It should be noted that all referenced works based on the *shifting paradigm concept* were developed using a gain-scheduled state-feedback controller. However, in some cases, the full state is not available, thus requiring the use of some other techniques, e.g., output-feedback control. The main goal of this work is to propose an LMI-based methodology for designing a *shifting* output-feedback controller for polytopic LPV systems subject to time-varying saturations, thus extending the methodology proposed in Ruiz et al. (2019) to the output-feedback case. The overall design approach is developed without considering the use of parameter-dependent QLF and the presence of external disturbances in order to keep the mathematical complexity somehow limited, and such extension will be addressed in future works.

The rest of the paper is organized as follows. Notation and some mathematical background is provided in Section 2. The

problem statement is formulated in Section 3. In Section 4, the LMI-based methodology for the controller design is given. In Section 5, simulation results are presented using a nonlinear quadrotor model. Finally, the main conclusions and perspectives on future research are outlined in Section 6.

2. NOTATION AND MATHEMATICAL BACKGROUND

This section presents the notation and relevant mathematical background to the rest of this paper.

2.1 Notation

The notations $\mathbb{R}$ and $\mathbb{R}_+$ stand for the set of real and non-negative real numbers, respectively. $\mathbb{N}$ corresponds to the set of natural numbers. The set of $n \times m$ real matrices is denoted as $\mathbb{R}^{n \times m}$ and the set of $n \times n$ symmetric real matrices is expressed as $\mathbb{S}^n$. For $M \in \mathbb{S}^n$, the notation $M \succ 0$ $(M \succeq 0)$ and $M \prec 0$ $(M \preceq 0)$ stand for a positive (semi-)definite matrix and for a negative (semi-)definite matrix, respectively. $M \in \mathbb{S}^n_+$ is used as a shorthand for positive-definite symmetric matrices in situations with limited space. The symbols I_n, $\text{diag}\{\ldots\}$, $\star$ and $\bullet$ represent the $n-$dimensional identity matrix, a block-diagonal matrix, the symmetric block in the LMIs and an element that has no influence on development, respectively. The transpose of a matrix M is denoted by M^T and the shorthand $He\{\cdot\} = (\cdot) + (\cdot)^T$ is used in situations with limited space. An element-wise inequality is represented by $\leq$. The subscripts a_i, $A_{\{i\}}$ and $A_{[i]}$ indicate the ith position of a vector, the ith vertex matrix and the ith row of the corresponding matrix, respectively. Finally, in some cases, the time dependency of time-varying variables is dropped to lighten the notation.

2.2 Polytopic representation

The polytopic representation of parameter-dependent matrices is used throughout this paper (Briat, 2014), where generic matrices such as $F(\vartheta(t))$, $G(\varphi(t))$ and $H(\vartheta(t), \varphi(t))$ with dependence on scheduling parameter vectors $\vartheta(t) \in \Theta \subset \mathbb{R}^{n_\vartheta}$ and $\varphi(t) \in \Phi \subset \mathbb{R}^{n_\varphi}$, with Θ and Φ known, bounded and closed polytopic sets, are defined as the convex combination of a finite set of N_Θ, N_Φ and $N_\Theta \times N_\Phi$ known vertex matrices $F_{\{i\}}$, $G_{\{j\}}$ and $H_{\{i,j\}}$, respectively, $\forall i = 1, \ldots, N_\Theta$ and $\forall j = 1, \ldots, N_\Phi$:

$$F(\vartheta) \triangleq \sum_{i=1}^{N_\Theta} \mu_i(\vartheta) F_{\{i\}}, \quad G(\varphi) \triangleq \sum_{j=1}^{N_\Phi} \eta_j(\varphi) G_{\{j\}},$$

$$H(\vartheta, \varphi) \triangleq \sum_{i=1}^{N_\Theta} \mu_i(\vartheta) H_{\{i\}}(\varphi) = \sum_{i=1}^{N_\Theta} \sum_{j=1}^{N_\Phi} \mu_i(\vartheta) \eta_j(\varphi) H_{\{i,j\}}, \tag{1}$$

where N_Θ and N_Φ denote the known number of vertices of the respective polytopes. $\mu(\vartheta) \in \mathscr{S}_\Theta$ and $\eta(\varphi) \in \mathscr{S}_\Phi$ are the known polytopic weight vectors fulfilling $\forall \vartheta \in \Theta$ and $\forall \varphi \in \Phi$, respectively, the unitary simplexes:

$$\mathscr{S}_\Theta \triangleq \left\{ \mu(\vartheta) \in \mathbb{R}^{N_\Theta} : \sum_{i=1}^{N_\Theta} \mu_i(\vartheta) = 1, \ \mu_i(\vartheta) \geq 0 \right\}, \tag{2}$$

$$\mathscr{S}_\Phi \triangleq \left\{ \eta(\varphi) \in \mathbb{R}^{N_\Phi} : \sum_{j=1}^{N_\Phi} \eta_j(\varphi) = 1, \ \eta_j(\varphi) \geq 0 \right\}. \tag{3}$$

2.3 Application of Pólya's relaxation theorem

Following Sala and Arino (2007), let us define $\mathbf{i} = (i_1, \ldots, i_p) \in \mathbb{N}^p$, for denoting a $p-$dimensional multi-index, and the sets $\mathbb{I}_{(p, N_\Theta)}$ and $\mathbb{I}^+_{(p, N_\Theta)}$ as:

$$\mathbb{I}_{(p, N_\Theta)} \triangleq \{ \mathbf{i} \in \mathbb{N}^p : 1 \leq i_k \leq N_\Theta, \ \forall k = 1, \ldots, p \}, \tag{4a}$$

$$\mathbb{I}^+_{(p, N_\Theta)} \triangleq \{ \mathbf{i} \in \mathbb{I}_{(p, N_\Theta)} : i_k \leq i_{k+1}, \ k = 1, \ldots, p-1 \}. \tag{4b}$$

Then, the following result holds.

Lemma 1. (Pólya's relaxation theorem). Consider the LMI:

$$\sum_{i_1=1}^{N_\Theta} \sum_{i_2=1}^{N_\Theta} \cdots \sum_{i_p=1}^{N_\Theta} \mu_{i_1}(\vartheta) \mu_{i_2}(\vartheta) \cdots \mu_{i_p}(\vartheta) \, x^T Q_{\{i_1, \ldots, i_p\}} x > 0,$$

$$\equiv \sum_{\mathbf{i} \in \mathbb{I}_{(p, N_\Theta)}} \mu_{\mathbf{i}}(\vartheta) x^T Q_{\{\mathbf{i}\}} x > 0, \tag{5}$$

and a chosen Pólya's relaxation degree $d \in \mathbb{N}$, with $d \geq 0$, such that the following set of LMIs is satisfied:

$$\sum_{\mathbf{k} \in \mathscr{P}(\mathbf{i})} Q_{\{\mathbf{k}\}} \succ 0, \quad \forall \mathbf{i} \in \mathbb{I}^+_{(p+d, N_\Theta)} \tag{6}$$

where $\mathscr{P}(i) \subset \mathbb{I}_{(p+d, N_\Theta)}$ corresponds to the set of permutations, with possible repeated elements, of the multi-index $\mathbf{i}$. Then, positive-definiteness of (5) is guaranteed with necessary conditions for large values of d, thus increasing the computational burden at the cost of reducing the overall conservatism.

3. PROBLEM STATEMENT

Let us consider the following continuous-time LPV system:

$$\begin{cases} \dot{x}_p(t) = A(\vartheta(t)) x_p(t) + B(\vartheta(t)) sat(u(t), \sigma(t)), \\ y(t) = C(\vartheta(t)) x_p(t), \end{cases} \tag{7}$$

where $x_p(t) \in \mathbb{R}^{n_x}$ is the plant state, $u(t) \in \mathbb{R}^{n_u}$ denotes the control input and $y(t) \in \mathbb{R}^{n_y}$ stands for the measured output. $A(\vartheta(t)) \in \mathbb{R}^{n_x \times n_x}$, $B(\vartheta(t)) \in \mathbb{R}^{n_x \times n_u}$ and $C(\vartheta(t)) \in \mathbb{R}^{n_y \times n_x}$ correspond to the state, input and output parameter-dependent matrices, respectively.

The input $u(t)$ in (7) is affected by a symmetric saturation function $sat(u(t), \sigma(t)) : \mathbb{R}^{n_u} \to \mathbb{R}^{n_u}$, defined as:

$$sat(u(t), \sigma(t)) = sign(u(t)) \min(|u(t)|, \sigma(t)), \tag{8}$$

where $\sigma(t) \in \mathbb{R}^{n_u}_+$ is a given vector that contains each instantaneous limit value $\sigma_h(t) \in \mathbb{R}_+ \ \forall h = 1, \ldots, n_u$. $\sigma_h(t)$ belongs to the interval $[\underline{\sigma}_h, \overline{\sigma}_h]$, with $\underline{\sigma}_h$ and $\overline{\sigma}_h$ as the lowest and highest possible saturation limits for each $u_h(t)$, respectively.

3.1 Shifting output-feedback controller structure

Following Ruiz et al. (2019), the controller's performance regulation is achieved by decreasing/increasing the convergence speed of the closed-loop system response through the scheduling vector $\varphi(t)$, for which a mapping with the possible instantaneous values of $\sigma(t)$ is established. Then, the fastest convergence speed of the closed-loop response is ensured when $\sigma(t) \to \overline{\sigma}$ and the slowest response when $\sigma(t) \to \underline{\sigma}$.

Let us define the structure of a *shifting* output-feedback controller as follows:

$$\begin{cases} \dot{x}_c(t) = A_c(\vartheta(t), \varphi(t)) x_c(t) + B_c(\vartheta(t), \varphi(t)) y(t), \\ u_c(t) = C_c(\vartheta(t), \varphi(t)) x_c(t) + D_c(\vartheta(t), \varphi(t)) y(t), \end{cases} \tag{9}$$

where $x_c(t) \in \mathbb{R}^{n_c}$ is the control state and $u_c(t) \in \mathbb{R}^{n_u}$ denotes the controller's output. $A_c(\vartheta(t), \varphi(t))$, $B_c(\vartheta(t), \varphi(t))$,

$C_c(\vartheta(t), \varphi(t))$ and $D_c(\vartheta(t), \varphi(t))$ correspond to the parameter-dependent controller matrices, with appropriate dimensions, to be designed.

3.2 Closed-loop performance criterion

Consider the augmented state $x = \begin{bmatrix} x_p^T, x_c^T \end{bmatrix}^T$ and the interconnection of (7) and (9) with $u = u_c$, thus defining the closed-loop LPV system dynamics as:

$$\dot{x} = \mathcal{A}(\vartheta, \varphi)x + \mathcal{B}(\vartheta)sat\left(\mathcal{K}(\vartheta, \varphi)x\right), \quad (10)$$

with

$$\mathcal{A}(\vartheta, \varphi) \triangleq \begin{bmatrix} A(\vartheta) & 0 \\ B_c(\vartheta, \varphi)C(\vartheta) & A_c(\vartheta, \varphi) \end{bmatrix}, \mathcal{B}(\vartheta) \triangleq \begin{bmatrix} B(\vartheta) \\ 0 \end{bmatrix}$$

and

$$\mathcal{K}(\vartheta, \varphi) \triangleq [D_c(\vartheta, \varphi)C(\vartheta) \ C_c(\vartheta, \varphi)].$$

Let us consider the following quadratic Lyapunov function (QLF):

$$V(x) \triangleq x^T P^{-1} x, \quad (11)$$

with $P \in \mathbb{S}_+^n$ as a Lyapunov matrix with dimension $n = n_x + n_c$. Thereupon, let us define the closed-loop performance criterion considered throughout this work based on the *shifting paradigm concept*, the closed-loop LPV system dynamics (10) and the above defined QLF (11), as follows:

Definition 1. (Guaranteed shifting decay rate). The LPV system (7) with the *shifting* output-feedback controller (9) is said to have a *guaranteed shifting decay rate* $\lambda(\vartheta, \varphi) \in \mathbb{R}_+$ if:

$$\dot{V}(x) \le -2\lambda(\vartheta, \varphi)V(x), \quad (12)$$

where $V(x)$ is a positive definite function.

3.3 Region constraints

The control input $u(t)$ is still affected by the nonlinear saturation function (8), complicating the obtention of computationally applicable design conditions. For this reason, it is important to ensure that $u(t)$ is within the linear region of the actuators $R_L(t) \subset \mathbb{R}^{n_u} \ \forall t \ge 0$, as defined by the symmetrical polyhedral set:

$$R_L(t) \triangleq \{u(t) \in \mathbb{R}^{n_u} : -\sigma(t) \le u(t) \le \sigma(t)\}, \quad (13)$$

which can be mapped onto the state-domain through the relationship $u(t) = \mathcal{K}(\vartheta(t), \varphi(t))x(t)$, thus obtaining:

$$R_L(\vartheta, \varphi) \triangleq \left\{x \in \mathbb{R}^n : |\mathcal{K}_{[h]}(\vartheta, \varphi)x| \le \sigma_h\right\}, \quad (14)$$

where $\mathcal{K}_{[h]}(\vartheta, \varphi) = \begin{bmatrix} D_{c[h]}(\vartheta, \varphi)C(\vartheta) & C_{c[h]}(\vartheta, \varphi) \end{bmatrix} \ \forall h = 1, \dots, n_u$.

Let us represent the square of the saturation limit variations $\sigma(t)^2$ using a given parameter-dependent vector function $\hat{\sigma}(\varphi(t)) \in \mathbb{R}_+^{n_u}$. Then, by following a procedure akin to the one proposed by Tarbouriech et al. (2011), the region $R_L(\vartheta, \varphi)$ can be rewritten $\forall h = 1, \dots, n_u$ as:

$$R_L(\vartheta, \varphi) \triangleq \left\{x \in \mathbb{R}^n : x^T \frac{\mathcal{K}_{[h]}(\vartheta, \varphi)^T \mathcal{K}_{[h]}(\vartheta, \varphi)}{\hat{\sigma}_h(\varphi)} x \le 1\right\}. \quad (15)$$

Thereupon, with the objective of guaranteeing $u(t) \in R_L(t)$, the following set of inclusions is established:

$$\mathscr{E}(X) \subset \mathscr{E}(P), \quad (16a)$$
$$\mathscr{E}(P) \subset R_L(\vartheta, \varphi), \quad (16b)$$

where $\mathscr{E}(X)$ and $\mathscr{E}(P)$ are hyper-ellipsoidal regions that correspond to the region of the state-space domain which contains

the initial conditions of interest $x(0)$ and the unit level curve of Lyapunov delimited by the QLF (11), respectively, and they are defined as follows:

$$\mathscr{E}(X) \triangleq \left\{x \in \mathbb{R}^n : x^T X^{-1} x \le 1\right\}, \quad (17)$$

$$\mathscr{E}(P) \triangleq \left\{x \in \mathbb{R}^n : x^T P^{-1} x \le 1\right\}, \quad (18)$$

where $X \in \mathbb{S}_+^n$ is a chosen matrix that contains the information about where the initial states $x(0)$ are expected to lie.

Hence, $u(t) \in R_L(t)$ can be guaranteed $\forall t > 0$ if the initial state $x(0) \in \mathscr{E}(X)$ and (16) is satisfied. As a consequence, $u(t)$ does not saturate $\forall t \ge 0$ and the closed-loop LPV system (10) can be reduced to:

$$\dot{x} = (\mathcal{A}(\vartheta, \varphi) + \mathcal{B}(\vartheta)\mathcal{K}(\vartheta, \varphi))x = A_{cl}(\vartheta, \varphi)x \quad (19)$$

for design purposes.

3.4 Problem definition

Finally, on the basis of the closed-loop performance criterion (*Definition 1*) and the region constraints established in (16), the problem considered in this work can be formulated as follows:

Problem 1. Given the LPV system (7) subject to the time-varying saturation (8), a *shifting* output-feedback controller (9), a guaranteed *shifting* decay rate $\lambda(\vartheta, \varphi)$, and the regions (15)-(18), find P and the parameter-dependent controller matrices $A_c(\vartheta, \varphi)$, $B_c(\vartheta, \varphi)$, $C_c(\vartheta, \varphi)$ and $D_c(\vartheta, \varphi)$ such that for any $x(0) \in \mathscr{E}(X)$ the closed-loop LPV system dynamics (10) satisfies (12).

4. SHIFTING OUTPUT-FEEDBACK CONTROLLER SYNTHESIS

Let us introduce the conditions for designing a dynamic output-feedback controller that ensures some desired guaranteed shifting decay rate. According to Chilali and Gahinet (1996); Scherer et al. (1997) and Tarbouriech et al. (2011), a change of control variables is needed, which is achieved by partitioning the Lyapunov matrices P and P^{-1}, as follows:

$$P \triangleq \begin{bmatrix} R & M \\ M^T & \bullet \end{bmatrix}, P^{-1} \triangleq \begin{bmatrix} S & N \\ N^T & \bullet \end{bmatrix}, \quad (20)$$

with $R, S \in \mathbb{S}_+^{n_x}$ and $N, M \in \mathbb{R}^{n_x \times n_c}$. Thereupon, from the identity $PP^{-1} = I_n$ the following relationship:

$$P \underbrace{\begin{bmatrix} I_n & S \\ 0 & N^T \end{bmatrix}}_{\Pi_S} = \underbrace{\begin{bmatrix} R & I_n \\ M^T & 0 \end{bmatrix}}_{\Pi_R} \quad (21)$$

is obtained with the congruence matrices Π_S and Π_R.

Using the given criterion in Definition 1, the following set of parameter-dependent LMIs and decision variables R, S, $\hat{A}_c(\vartheta, \varphi) \in \mathbb{R}^{n_c \times n_c}$, $\hat{B}_c(\vartheta, \varphi) \in \mathbb{R}^{n_c \times n_y}$, $\hat{C}_c(\vartheta, \varphi) \in \mathbb{R}^{n_u \times n_c}$ and $\hat{D}_c(\vartheta, \varphi) \in \mathbb{R}^{n_u \times n_y}$ are derived by considering the closed-loop LPV system (19), the shifting output-feedback (9), the QLF (11) with a given guaranteed shifting decay rate $\lambda(\vartheta, \varphi) \in \mathbb{R}_+$ and the relationship (21):

$$\begin{bmatrix} R & I_n \\ I_n & S \end{bmatrix} \succ 0, \quad (22)$$

$$He\left\{\begin{bmatrix} \Upsilon_{11}(\vartheta, \varphi) & \Upsilon_{12}(\vartheta, \varphi) \\ \Upsilon_{21}(\vartheta, \varphi) & \Upsilon_{22}(\vartheta, \varphi) \end{bmatrix}\right\} + 2\lambda(\vartheta, \varphi)\begin{bmatrix} R & I_n \\ I_n & S \end{bmatrix} \prec 0, \quad (23)$$

where the block elements of $\Upsilon(\vartheta, \varphi)$ are defined as:

$$
\begin{aligned}
\Upsilon_{11}(\vartheta, \varphi) &\triangleq A(\vartheta)R + B(\vartheta)\hat{C}_c(\vartheta, \varphi), \\
\Upsilon_{12}(\vartheta, \varphi) &\triangleq A(\vartheta) + B(\vartheta)\hat{D}_c(\vartheta, \varphi)C(\vartheta), \\
\Upsilon_{21}(\vartheta, \varphi) &\triangleq \hat{A}_c(\vartheta, \varphi), \\
\Upsilon_{22}(\vartheta, \varphi) &\triangleq SA(\vartheta) + \hat{B}_c(\vartheta, \varphi)C(\vartheta),
\end{aligned} \tag{24}
$$

with:

$$
\begin{aligned}
\begin{bmatrix} \hat{A}_c(\vartheta, \varphi) & \hat{B}_c(\vartheta, \varphi) \\ \hat{C}_c(\vartheta, \varphi) & \hat{D}_c(\vartheta, \varphi) \end{bmatrix} &= \begin{bmatrix} SA(\vartheta)R & 0 \\ 0 & 0 \end{bmatrix} + \begin{bmatrix} N & SB(\vartheta) \\ 0 & I_n \end{bmatrix} \\
&\times \begin{bmatrix} A_c(\vartheta, \varphi) & B_c(\vartheta, \varphi) \\ C_c(\vartheta, \varphi) & D_c(\vartheta, \varphi) \end{bmatrix} \begin{bmatrix} M^T & 0 \\ C(\vartheta)R & I_n \end{bmatrix}.
\end{aligned} \tag{25}
$$

Then, if constraints (22) and (23) are satisfied, the closed-loop LPV response (19) guarantees (12). Furthermore, the parameter-dependent controller matrices in (9) can be computed from the decision variables (25) subject to the condition $MN^T = I_n - RS$.

Remark 1. If matrices M and N have full row rank, then the computation of $A_c(\vartheta, \varphi)$, $B_c(\vartheta, \varphi)$, $C_c(\vartheta, \varphi)$ and $D_c(\vartheta, \varphi)$ through the decision matrices appearing in (25) is always possible (Chilali and Gahinet, 1996). Furthermore, the parameter-dependent controller matrices in (9) are uniquely determined if $n_x = n_c$, thus implying that N and M are nonsingular square matrices.

Let us provide the conditions that ensure the convergence to zero of any state trajectory $x(t)$ starting in the region $\mathscr{E}(P)$. The set of inclusions (16) forces the state trajectory to remain in $R_L(\vartheta, \varphi)$ where the nonlinear saturation function (8) is not triggered. By defining the region:

$$
\mathscr{E}(X_0) \triangleq \left\{ x_p \in \mathbb{R}^{n_x} : x_p^T X_0^{-1} x_p \leq 1 \right\}, \tag{26}
$$

where $X_0 \in \mathbb{S}_+^{n_x}$ is a chosen matrix that contains the information about where the initial states $x_p(0)$ are expected to lie, $x_p(0) \in \mathscr{E}(X_0)$ ensures that any state trajectory $x(t) \in \mathscr{E}(P) \; \forall t \geq 0$ under the assumption that $x_c(0) = 0$, which is introduced to avoid that the matrices M and N appear as decision variables in the LMIs. Hence, the inclusion (16a) is modified as:

$$
\mathscr{E}(X_0) \subset \mathscr{E}(P)|_{(x(0),0)}. \tag{27}
$$

By considering the partition of P^{-1} in (20), the inclusion (27), and the regions mentioned in (18) and (26) with a given matrix X_0, the following LMI is generated:

$$
X_0^{-1} - S \succeq 0. \tag{28}
$$

Furthermore, the parameter-dependent LMI (29) is obtained $\forall h = 1, \ldots, n_u$ from the inclusion (16b), the relationship (21), the regions (15) and (18), and a given parameter-dependent vector function $\hat{\sigma}(\varphi) \in \mathbb{R}_+^{n_u}$:

$$
\begin{bmatrix} \hat{\sigma}_h(\varphi) & \hat{C}_{c[h]}(\vartheta, \varphi) & \hat{D}_{c[h]}(\vartheta, \varphi)C(\vartheta) \\ \star & R & I_n \\ \star & \star & S \end{bmatrix} \succeq 0. \tag{29}
$$

Then, if constraints (22), (23), (28) and (29) are fulfilled, the convergence of $x(t) \to 0$ when $t \to \infty$ is guaranteed for any $x_p(0) \in \mathscr{E}(X_0)$. Furthermore, $u(t) \in R_L(t)$.

Note that conditions (23) and (29) represent an infinite number of constraints. To this end, the polytopic representation (1)-(3) and Lemma 1 are applied to (23) and (29), respectively, thus obtaining a finite number of LMIs $\forall j = 1, \ldots, N_\Phi$:

$$
\sum_{\mathbf{k} \in \mathscr{P}(\mathbf{i})} \Xi_{\{\mathbf{k}, j\}} \prec 0, \quad \forall \mathbf{i} \in \mathbb{I}_{(3+d_1, N_\Theta)}^+, \tag{30}
$$

and $\forall h = 1, \ldots, n_u$, $\forall \mathbf{l} \in \mathbb{I}_{(2+d_2, N_\Theta)}^+$:

$$
\sum_{\mathbf{m} \in \mathscr{P}(\mathbf{l})} \left(\begin{bmatrix} \hat{\sigma}_{h\{j\}} & \hat{C}_{c[h],\{m_1,j\}} & \hat{D}_{c[h],\{m_1,j\}}C_{\{m_2\}} \\ \star & R & I_n \\ \star & \star & S \end{bmatrix} \right) \succeq 0, \tag{31}
$$

where $d_1, d_2 \in \mathbb{N}_{\geq 0}$ and $\Xi_{\{\mathbf{k}, j\}}$ is defined as:

$$
\begin{aligned}
He &\left\{ \begin{bmatrix} A_{\{k_1\}}R + B_{\{k_1\}}\hat{C}_{c,\{k_2,j\}} & A_{\{k_1\}} + B_{\{k_1\}}\hat{D}_{c,\{k_2,j\}}C_{\{k_3\}} \\ \hat{A}_{c,\{k_1,j\}} & SA_{\{k_1\}} + \hat{B}_{c,\{k_1,j\}}C_{\{k_2\}} \end{bmatrix} \right\} \\
&+ 2\lambda_{\{k_1,j\}} \begin{bmatrix} R & I_n \\ I_n & S \end{bmatrix}.
\end{aligned}
$$

Then, (12) holds for all parameter-dependent matrices given in (7), (9) and the parameter-dependent vector in (15).

5. ILLUSTRATIVE EXAMPLE

Consider the attitude model of a quadrotor taken from Trapiello et al. (2019) with parameters as described in Rubí et al. (2019), and under the assumption of negectable gyroscopic effect. Then, the system (7) is characterized by the parameters in Table 1, $x_p(t) = [\dot{\phi}(t), \dot{\theta}(t), \dot{\psi}(t), \phi(t), \theta(t), \psi(t)]^T$ and the moments produced by the rotors $u(t)$, as follows:

$$
u(t) = \begin{bmatrix} u_1(t) \\ u_2(t) \\ u_3(t) \end{bmatrix} = \begin{bmatrix} lk_T(\Omega_4(t)^2 - \Omega_2(t)^2) \\ lk_T(\Omega_3(t)^2 - \Omega_1(t)^2) \\ k_Q \sum_{i=1}^4 (-1)^i \Omega_i(t)^2 \end{bmatrix}. \tag{32}
$$

The selected scheduling vector is $\vartheta(t) = [\dot{\phi}(t), \dot{\theta}(t)]$ with $\dot{\phi}(t), \dot{\theta}(t) \in [-1, 1]$, thus defining the polytope with $N_\Theta = 4$ vertices that contains the following parameter-dependent system matrices (7):

$$
A(\vartheta(t)) = \begin{bmatrix} 0 & 0 & a_{13}(\cdot) & \\ 0 & 0 & a_{23}(\cdot) & 0_{3\times3} \\ a_{31}(\cdot) & a_{32}(\cdot) & 0 & \\ \hline & I_3 & & 0_{3\times3} \end{bmatrix} \tag{33}
$$

$$
B(\vartheta(t)) = \begin{bmatrix} J^{-1} \\ 0_{3\times3} \end{bmatrix}, \; C(\vartheta(t)) = [0_{3\times3} \; I_3],
$$

where $a_{13}(\vartheta_2(t)) = \vartheta_2(t)\frac{J_{22}-J_{33}}{J_{11}}$, $a_{13}(\vartheta_2(t)) = \vartheta_1(t)\frac{J_{33}-J_{11}}{J_{22}}$, $a_{31}(\vartheta_2(t)) = \vartheta_2(t)\frac{J_{11}-J_{22}}{2J_{33}}$, $a_{32}(\vartheta_1(t)) = \vartheta_1(t)\frac{J_{11}-J_{22}}{2J_{33}}$ and $J = diag\{J_{11}, J_{22}, J_{33}\}$.

Table 1. Parameter symbol descriptions.

Symbol	Description	Units
$\phi(t), \theta(t), \psi(t)$	Euler angles.	rad
$\dot{\phi}(t), \dot{\theta}(t), \dot{\psi}(t)$	Euler angle rates.	$\mathrm{rad\,s^{-1}}$
l	Distance from the rotor to the CoG.	m
k_T	Thrust coefficient.	$\mathrm{N\,rpm^{-2}}$
k_Q	Torque coefficient.	$\mathrm{N\,m\,rpm^{-2}}$
Ω_i	Angular speed of the $i-th$ propeller.	rpm
Ω_0	Fixed minimum propeller speed.	rpm
J	Body moment of inertia matrix.	$\mathrm{kg\,m^2}$

5.1 Time-varying input saturations

Under the assumption that all rotors share the same behaviour regarding saturation, let us consider $\forall i = 1, \ldots, 4$ that $\Omega_i \in [\Omega_0, \Delta_\Omega(t)]$ where Ω_0 is fixed to 1075 (rpm) and $\Delta_\Omega(t)$ is a known function that describes the instantaneous maximum propeller speed, which varies due to the discharge of the battery. Then, it is also assumed that $\Delta_\Omega(t)$ varies within the interval

$[\Delta_{\underline{\Omega}}, \Delta_{\overline{\Omega}}]$ with $\Omega_0 < \Delta_{\underline{\Omega}} < \Delta_{\overline{\Omega}}$, $\Delta_{\underline{\Omega}} = 5000$ (rpm) and $\Delta_{\overline{\Omega}} = 8600$ (rpm), respectively.

In order to handle the propeller speed limitation, let us define the largest available positive control action through Eq. (32) as follows:

$$\sigma_1(t) = \sigma_2(t) = lk_T(\Delta_\Omega(t)^2 - \Omega_0^2),$$
$$\sigma_3(t) = 2k_Q(\Delta_\Omega(t)^2 - \Omega_0^2),$$
$$\tag{34}$$

where $\sigma_1(t), \sigma_2(t) \in lk_T[(\Delta_{\underline{\Omega}}^2 - \Omega_0^2), (\Delta_{\overline{\Omega}}^2 - \Omega_0^2)]$ and $\sigma_3(t) \in 2k_Q[(\Delta_{\underline{\Omega}}^2 - \Omega_0^2), (\Delta_{\overline{\Omega}}^2 - \Omega_0^2)]$.

Then, let us introduce the performance scheduling parameter $\varphi(t) \in [0, 1]$, which is linked to the time-varying saturation function (8) and the limits described in (34) for the inputs $u_1(t)$, $u_2(t)$ and $u_3(t)$, respectively, as follows:

$$\varphi(t) = \frac{\overline{\sigma}_1^2 - \sigma_1(t)^2}{\overline{\sigma}_1^2 - \underline{\sigma}_1^2} = \frac{\overline{\sigma}_2^2 - \sigma_2(t)^2}{\overline{\sigma}_2^2 - \underline{\sigma}_2^2} = \frac{\overline{\sigma}_3^2 - \sigma_3(t)^2}{\overline{\sigma}_3^2 - \underline{\sigma}_3^2}. \tag{35}$$

Note that $\varphi(t)$ is a unique scheduling parameter due to the fact that $\sigma_h(t) \to \underline{\sigma}_h$ and $\sigma_h(t) \to \overline{\sigma}_h$ $\forall h = 1,2,3$ when the function $\Delta_\Omega(t) \to \Delta_{\underline{\Omega}}$ and $\Delta_\Omega(t) \to \Delta_{\overline{\Omega}}$, respectively. Thus, allowing to establish the following mapping:

$$\sigma_h(t)^2 \triangleq \hat{\sigma}_h(\varphi(t)) = \overline{\sigma}_h^2 + \varphi(t)\left(\underline{\sigma}_h^2 - \overline{\sigma}_h^2\right), \tag{36}$$

and, hence, $N_\Phi = 2$ and the corresponding vertices of $\hat{\sigma}(\varphi)$:

$$\hat{\sigma}_{\{1\}} = \left[\overline{\sigma}_1^2,\ \overline{\sigma}_2^2,\ \overline{\sigma}_3^2\right]^T, \quad \hat{\sigma}_{\{2\}} = \left[\underline{\sigma}_1^2,\ \underline{\sigma}_2^2,\ \underline{\sigma}_3^2\right]^T. \tag{37}$$

5.2 Design specifications

Consider that the initial attitude of the vehicle $\phi(0)$, $\theta(0)$ and $\psi(0)$ belongs to the interval $[-0.0873, 0.0873]$ (rad) and each Euler angle rate $\dot{\phi}(0)$, $\dot{\theta}(0)$ and $\dot{\psi}(0)$ is expected to lie in $[-0.0017, 0.0017]$ (rad s^{-1}), thus determining:

$$X_0^{-1} \triangleq \frac{1}{n_x}\,\mathrm{diag}\left\{\overline{\dot{\phi}}(0), \overline{\dot{\theta}}(0), \overline{\dot{\psi}}(0), \overline{\phi}(0), \overline{\theta}(0), \overline{\psi}(0)\right\}^{-2}. \tag{38}$$

Then, let us define the desired decay rate values of $\lambda(\vartheta, \varphi)$ taking into account the polytopic representation (1)-(3) with the purpose of regulating the convergence speed of (19) online:

$$\lambda_{i,1} = 3.18,\ \lambda_{i,2} = 0,\ \forall i = 1, \dots, 4. \tag{39}$$

Remark 2. Note that values of $\lambda_{i,1}$ in (39) can be obtained by using, e.g., linear search techniques or the bisection algorithm until Problem 1 becomes unfeasible.

Once the design specifications are defined, two Pólya's relaxation degree $d_1 = 1$ and $d_2 = 2$ are chosen and Problem 1 is solved through (22), (28), (30) and (31) using the SeDuMi solver (Sturm, 1999) and the YALMIP toolbox (Löfberg, 2004).

5.3 Performance illustration

The closed-loop performance of the designed controller is tested in a scenario without the presence of external disturbances and under three different saturation limits that remain constant during the simulation for illustrative purposes. To this end, each instantaneous saturation limit is fixed to $\sigma_h(t)^2 = \{\overline{\sigma}_h^2, 0.5(\overline{\sigma}_h^2 + \underline{\sigma}_h^2), \underline{\sigma}_h^2\}$ $\forall h = 1,2,3$ leading to the frozen values of $\varphi = \{0, 0.5, 1\}$ through the relationship (35). Furthermore, the controlled system is simulated with $x(0) = [0, 0, 0, 0.0524, -0.0349, 0.0175]^T$ and $x_c(0) = 0$.

Figs. 1-2 show the closed-loop response of the Euler angles and the controller states, respectively. Note that in both cases

the fastest closed-loop convergence speed, denoted by a red line, corresponds to $\sigma_h(t) = \overline{\sigma}_h$ implying $\varphi = 0$. Conversely, it can be seen that the slowest closed-loop response occurs when $\sigma_h(t) \to \underline{\sigma}_h$, which corresponds to $\varphi = 1$. This demonstrates the adaptability of the designed *shifting* output-feedback controller regarding the closed-loop convergence speed. Furthermore, it is also shown that the controller achieves the closed-loop system stabilization.
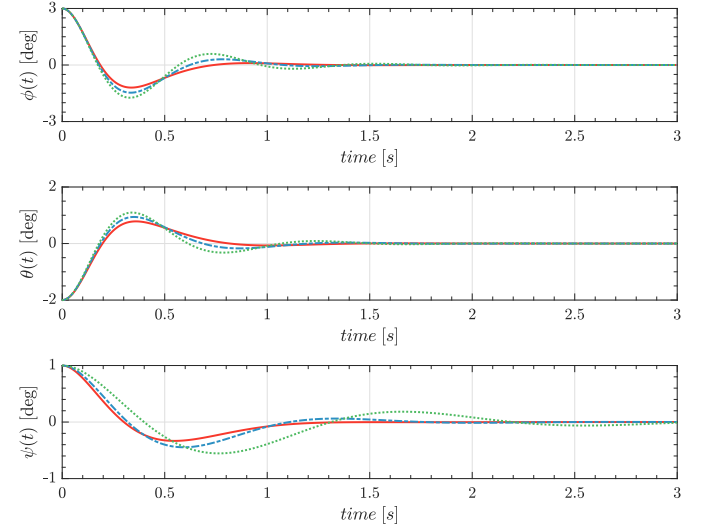

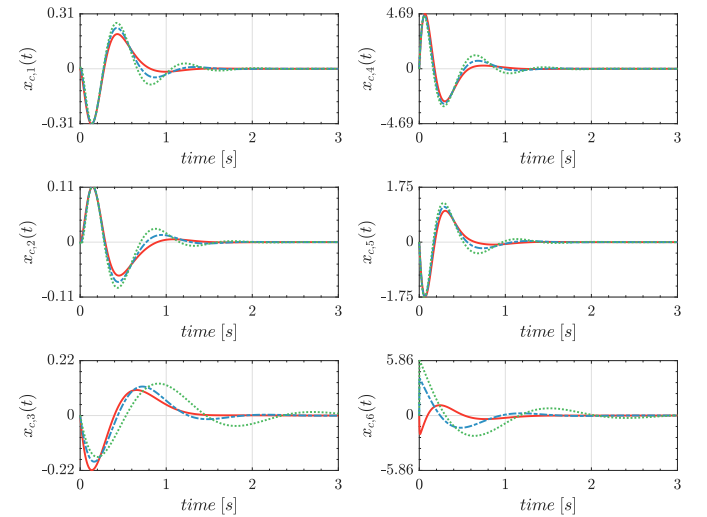Fig. 1. Closed-loop Euler angle responses. ($\phi = 0$ (——), $\phi = 0.5$ (– · –) and $\phi = 1$ (······).)

Fig. 2. Controller states behaviour. ($\phi = 0$ (——), $\phi = 0.5$ (– · –) and $\phi = 1$ (······).)

Finally, Fig. 3 shows the evolution of the control actions over time for the three frozen values of φ where, for illustrative purposes, the instantaneous saturation limits of each control signal $u_h(t)$ $\forall h = 1,2,3$ are not plotted. Furthermore, it can be seen that $u(t)$ remains inside the boundaries established by all the mentioned values of $\sigma(t)$.

6. CONCLUSIONS

In this paper, the problem of designing a *shifting* output-feedback controller for polytopic LPV systems subject to time-
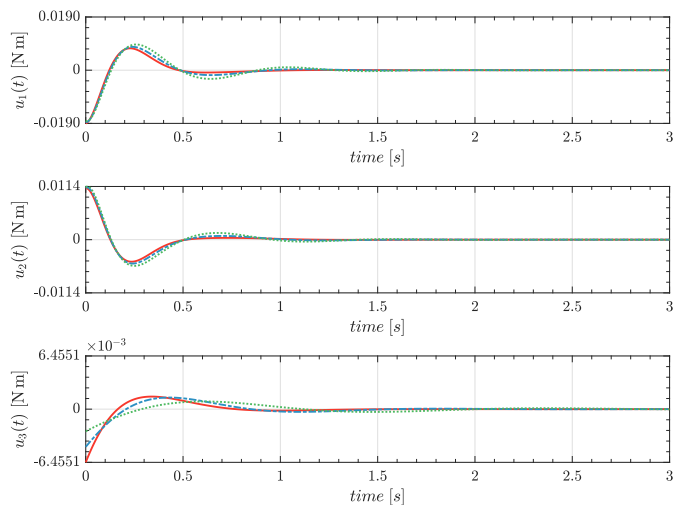
Fig. 3. Evolution of the control inputs. ($\phi = 0$ (——), $\phi = 0.5$ (– · –), $\phi = 1$(· · · · ·), $\sigma_1 = \sigma_2 = \{0.885, 0.659, 0.29\}\,(\mathrm{N\,m})$ and $\sigma_3 = \{0.147, 0.109, 0.048\}\,(\mathrm{N\,m})$.)

varying saturations has been investigated. The design procedure proposed in Ruiz et al. (2019) has been extended to the output-feedback case through the use of a QLF, the invariant ellipsoidal theory and the use of the *shifting paradigm concept*, thus obtaining a suitable set of LMIs that can be solved via the available solvers. Furthermore, due to the appearance of multiple polytopic summations, the Pólya's relaxation theorem has been used to reduce the complexity in the design stage.

The results obtained in the illustrative example show that the guaranteed *shifting* decay rate performance criterion is satisfied by the controller. This controller adapts online the closed-loop response in sense of convergence speed according to the saturation limit values of the actuators. Future work will incorporate into the proposed method the quadratic boundedness framework, parameter-dependent QLFs, and robust techniques.

REFERENCES

Abdilla, A., Richards, A., and Burrow, S. (2015). Endurance optimisation of battery-powered rotorcraft. In C. Dixon and K. Tuyls (eds.), *Towards Autonomous Robotic Systems*, 1–12. Springer International Publishing, Cham.

Briat, C. (2014). Linear parameter-varying and time-delay systems. *Analysis, observation, filtering & control*, 3, 5–7.

Cao, Y.Y., Lin, Z., and Shamash, Y. (2002). Set invariance analysis and gain-scheduling control for LPV systems subject to actuator saturation. *Systems & Control Letters*, 46(2), 137–151.

Chilali, M. and Gahinet, P. (1996). H_∞ design with pole placement constraints: an LMI approach. *IEEE Transactions on automatic control*, 41(3), 358–367.

da Silva, J. and Tarbouriech, S. (2005). Antiwindup design with guaranteed regions of stability: an LMI-based approach. *IEEE Transactions on Automatic Control*, 50(1), 106–111.

de Souza, C., Leite, V.J.S., Tarbouriech, S., and Castelan, E.B. (2021). Emulation-based dynamic output-feedback control of saturating discrete-time LPV systems. In *2021 American Control Conference (ACC)*, 1076–1081.

Faessler, M., Falanga, D., and Scaramuzza, D. (2017). Thrust mixing, saturation, and body-rate control for accurate aggressive quadrotor flight. *IEEE Robotics and Automation Letters*, 2(2), 476–482.

Hoffmann, G., Huang, H., Waslander, S., and Tomlin, C. (2007). Quadrotor helicopter flight dynamics and control: Theory and experiment. In *AIAA Guidance, Navigation and Control Conference and Exhibit*, 6461.

Kapila, V., Sparks, A.G., and Pan, H. (2001). Control of systems with actuator saturation non-linearities: An LMI approach. *International Journal of Control*, 74(6), 586–599.

Löfberg, J. (2004). YALMIP : A toolbox for modeling and optimization in MATLAB. In *2004 IEEE International Conference on Robotics and Automation (IEEE Cat. No.04CH37508)*, 284–289.

Nguyen, A.T., Zhang, H., Sentouh, C., and Popieul, J.C. (2018). Input-constrained LPV output feedback control for path following of autonomous ground vehicles. In *2018 Annual American Control Conference (ACC)*, 3233–3238.

Rotondo, D., Nejjari, F., and Puig, V. (2015). Design of parameter-scheduled state-feedback controllers using shifting specifications. *Journal of the Franklin Institute*, 352(1), 93–116.

Rubí, B., Ruiz, A., Peréz, R., and Morcego, B. (2019). Pathflyer: A benchmark of quadrotor path following algorithms. In *2019 IEEE 15th International Conference on Control and Automation (ICCA)*, 633–638.

Ruiz, A., Rotondo, D., and Morcego, B. (2019). Design of state-feedback controllers for linear parameter varying systems subject to time-varying input saturation. *Applied Sciences*, 9(17), 3606.

Ruiz, A., Rotondo, D., and Morcego, B. (2021). Design of shifting state-feedback controllers for LPV systems subject to time-varying saturations via parameter-dependent Lyapunov functions. *ISA Transactions*.

Sala, A. and Arino, C. (2007). Asymptotically necessary and sufficient conditions for stability and performance in fuzzy control: Applications of Pólya's theorem. *Fuzzy Sets and Systems*, 158(24), 2671–2686.

San-Miguel, A., Puig, V., and Alenyà, G. (2021). Disturbance observer-based LPV feedback control of a N-DoF robotic manipulator including compliance through gain shifting. *Control Engineering Practice*, 115, 104887.

Scherer, C., Gahinet, P., and Chilali, M. (1997). Multiobjective output-feedback control via LMI optimization. *IEEE Transactions on automatic control*, 42(7), 896–911.

Scorletti, G., Folcher, J.P., and El Ghaoui, L. (2001). Output feedback control with input saturations: LMI design approaches. *European Journal of Control*, 7(6), 567–579.

Sturm, J.F. (1999). Using SeDuMi 1.02, a MATLAB toolbox for optimization over symmetric cones. *Optimization methods and software*, 11(1-4), 625–653.

Tarbouriech, S., Garcia, G., da Silva Jr, J.M.G., and Queinnec, I. (2011). *Stability and stabilization of linear systems with saturating actuators*. Springer Science & Business Media.

Trapiello, C., Puig, V., and Morcego, B. (2019). Position-heading quadrotor control using LPV techniques. *IET Control Theory & Applications*, 13(6), 783–794.

Ungurán, R., Petrović, V., Pao, L.Y., and Kühn, M. (2019). Smart rotor control of wind turbines under actuator limitations. In *2019 American Control Conference (ACC)*, 3474–3481.

Wu, F., Grigoriadis, K.M., and Packard, A. (2000). Antiwindup controller design using linear parameter-varying control methods. *International Journal of Control*, 73(12), 1104–1114.